PROCEEDINGS OF SCIENCE

Recent charm results in the QCD medium from LHCb

Chenxi Gu[a,*] **for the LHCb collaboration**

[a] *Tsinghua University,*
Hai Dian, Beijing, China

E-mail: chenxi.gu@cern.ch

The forward acceptance of the LHCb detector allows proton and ion collisions to be probed in a unique kinematic range, complementary to the other LHC experiments. In this contribution we present some of the most recent charm results in proton-lead collisions at $\sqrt{s_{NN}}$ =8.16 TeV. We will discuss suppression of prompt D^0 production in the forward rapidity region, enhancement of double parton scattering, and the first measurement of prompt χ_{c1} and χ_{c2} production in pPb collisions at the LHC.

**** The European Physical Society Conference on High Energy Physics (EPS-HEP2021), ****
**** 26-30 July 2021 ****
**** Online conference, jointly organized by Universität Hamburg and the research center DESY ****

*Speaker

PoS(EPS-HEP2021)290

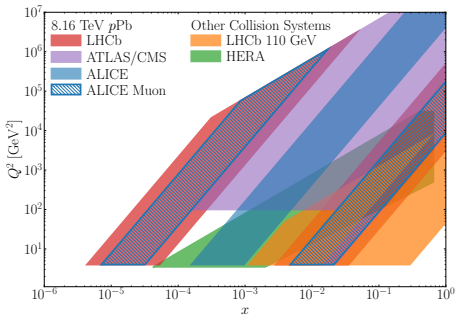

Figure 1: Q^2 and x coverage of LHCb acceptance.

1. Introduction

Proton-nucleus collisions provide an ideal platform to study cold nuclear matter effects without effects of quark gluon plasma (QGP). Heavy quark production is a valuable probe for such study. Two kinds of cold nuclear matter effects are considered in this contribution, including modification of parton distribution functions (nPDFs) inside the nucleus [1] and quarkonium suppression due to interactions with comoving particles.

LHCb has unique advantages for such research. The high-precision tracking system provides excellent vertex and momentum resolution [2, 3] and permits separation of prompt and b-decay components. LHCb's forward rapidity coverage allows access to the low Bjorken-x region inside the nucleus [4]. A diagram of the Q^2 and x coverage of the LHCb detector is shown in Fig.1.

The data sample was collected with the LHCb detector at the end of 2016 in two different configurations: forward collisions (p beam coming from upstream of VELO) and backward collisions (p beam coming from downstream of VELO), corresponding to an integrated luminosity of 12.2 ± 0.3 nb^{-1} and 18.6 ± 0.5 nb^{-1}, respectively. The proton beam energy was 6500 GeV and lead beam energy was 2560 GeV/nucleon.

2. Recent charm results in pPb collisions from LHCb

2.1 Prompt D^0 meson production in pPb collisions at $\sqrt{s_{NN}}$ =8.16 TeV

The D^0 candidates are reconstructed through $D^0 \to K^{\mp}\pi^{\pm}$ decays. Inclusive D^0 yield are extracted from fits to the $K^{\mp}\pi^{\pm}$ invariant mass spectrum. The prompt D^0 and beauty decay D^0 are separated via the impact parameter, which is the perpendicular distance from the primary vertex to D^0 path. D^0 mesons with a smaller impact parameter are more likely to originate from the primary interaction vertex. The precise D^0 measurement provides significant inputs to nPDFs at very small x region [5].

The forward-backward production ratio is defined as:

$$R_{\mathrm{FB}}\left(p_{\mathrm{T}}, y^*\right) \equiv \frac{\mathrm{d}^2\sigma_{p\mathrm{Pb}}\left(p_{\mathrm{T}}, +|y^*|\right)/\mathrm{d}p_{\mathrm{T}}\mathrm{d}y^*}{\mathrm{d}^2\sigma_{\mathrm{Pb}p}\left(p_{\mathrm{T}}, -|y^*|\right)/\mathrm{d}p_{\mathrm{T}}\mathrm{d}y^*} \tag{1}$$

which is calculated in the common rapidity bins between the forward and backward configuration, $2.5 < |y^*| < 4.0$. y^* is defined in the nucleon-nucleon center-of-mass frame.

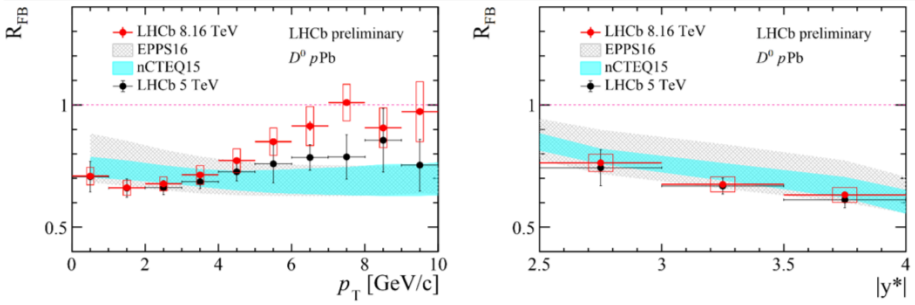

Figure 2: $R_{\rm FB}$ as a function of $p_{\rm T}$ (left) and y (right) in pPb data at $\sqrt{s_{NN}}$ = 8.16TeV

The forward to backward ratio is shown in Fig.2. The $R_{\rm FB}$ points show an increasing trend with $p_{\rm T}$, consistent with the measurement at 5TeV. The agreement with theoretical nPDF calculations is good in the low-$p_{\rm T}$ bins, while a discrepancy appears in high-$p_{\rm T}$ bins. The measurement of $R_{\rm FB}$ shown in the right plot of Fig.2 shows a slight dependence on rapidity, and the result agrees with the measurement at 5TeV and theoretical calculations. The $R_{\rm FB}$ values are dominated by data in the low $p_{\rm T}$ bins, which agree with the nPDF calculations. Although the data are higher than the calculations in high-$p_{\rm T}$ bins, they do not contribute significantly to the $p_{\rm T}$-integrated result of Fig.2.

2.2 Charm pair production and enhanced DPS in pPb collisions at $\sqrt{s_{NN}}$ =8.16TeV

In proton-ion collisions, DPS (double parton scattering) cross section is enhanced compared to SPS (single parton scattering) due to collisions of partons from two different nucleons in the ion, and the enhancement factor is about 3 in pPb collisions [6]. Two open charm hadrons D_1D_2 and $J/\psi D$ meson pairs are perfect tools to study this enhancement.For the opposite-sign pair, such as $D^0\bar{D}^0$, two hadrons have the opposite charm flavor. For the like-sign pair, such as D^0D^0, two hadrons have the same charm flavor.

In Fig.3, the invariant-mass distribution shows hints of differences between LS and OS pairs, and the $\Delta\phi$ distribution also shows some differences between LS and OS pairs. For OS pairs a near side peak is observed, suggesting OS pairs are correlated. The OS correlation is predicted to be sensitive to the properties of the hot medium formed in ultra-relativistic heavy nucleus-nucleus collisions [7, 8]. LS pairs produced in a DPS process are expected to be uncorrelated. Since DPS production involves two partons, it is very sensitive to the nuclear PDF (nPDF) in proton-ion collisions, including its possible dependence on the position inside the nucleus [9]. As shown in Fig.4, LS/OS ratios suggests DPS/SPS is enhanced by a factor approximately 3 in pPb compared to pp. The $\sigma_{\text{eff, }p\text{Pb}}$ result is different between pPb and Pbp data and between $J/\psi D^0$ and D^0D^0 pairs and it may suggest additional effects may be present, which can be further investigated using future LHCb data samples.

This is the first measurement of associated production of two charm hadrons in proton-lead collisions. The results confirm the predicted enhancement of double parton scattering production in proton-lead collisions compared to the single parton scattering production.

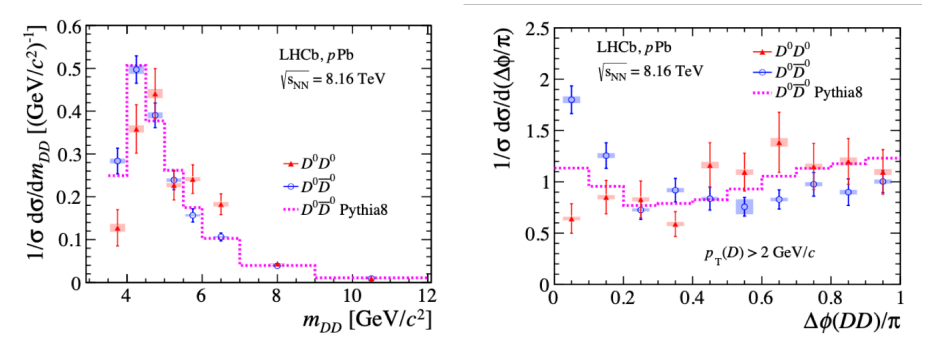

Figure 3: Two-charm hadron invariant-mass distribution (left) and $\Delta\phi$ distribution (right)

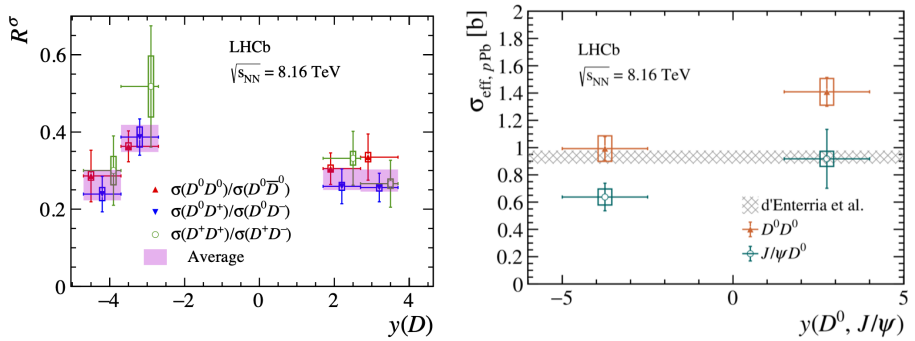

Figure 4: LS/OS differential cross-sections ratio (left) and effective cross-section (right)

2.3 Prompt cross-section ratio of χ_{c1}/χ_{c2} in pPb collisions at $\sqrt{s_{NN}}$ =8.16TeV

This first measurement of P-wave charmonia in nuclear collisions at the LHC uses pseudo decay time to separate the prompt component from the component produced in b decays. The χ_{cj} are reconstructed via $J/\psi\gamma$, where the J/ψ decays to $\mu\mu$. We can classify the event by photon reconstruciton technique: converted photons are reconstructed using the tracking system, with high momentum resolution, while calorimetric photons are reconstructed in the electromagnetic calorimeters, with a larger data sample. The mass-difference spectra are shown in Fig.5.

The cross-section ratio $\sigma\,(\chi_{c2})\,/\sigma\,(\chi_{c1})$ for the converted sample and calorimetric sample are shown in Fig.6, and are compared with results of the converted sample in pp collisions at 7 TeV [10]. The results are consistent with pp values for both forward and backward rapidity regions, within uncertainties. This suggests that the final-state nuclear effects impact the χ_{c1} and χ_{c2} states similarly within the achieved precision.

3. Summary and outlook

In this contribution, we demonstrate the unique capabilities of the LHCb detector to study CNM effects in heavy-ion collisions. Lots of analyses are in progress, such as open charm in pPb and Λ_c in PbPb. Furthermore, the LHCb detector is undergoing a major upgrade. In the future we expect more statistics in collider mode (pPb,PbPb), and SMOG2 will bring the fixed-target mode to a new energy and kinematic regions.

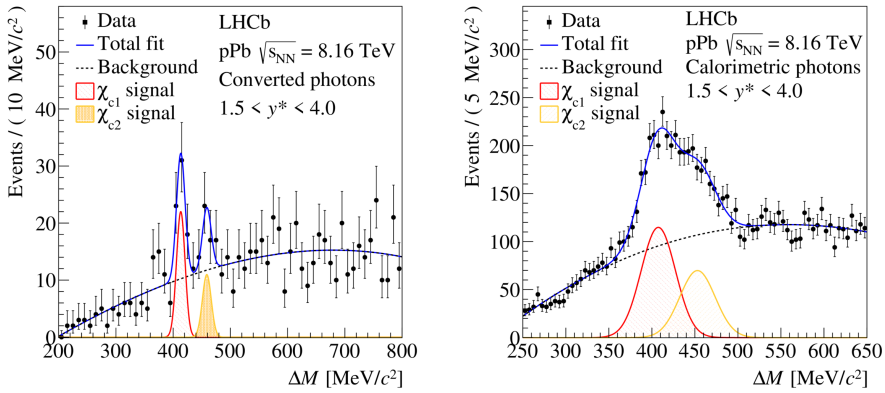

Figure 5: Mass-difference spectra of converted candidates (left) and calorimetric candidates (right)

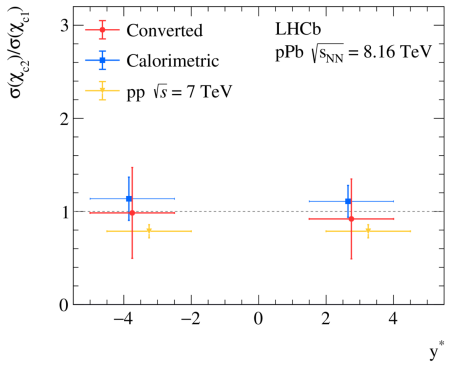

Figure 6: The cross-section ratio, $\sigma(\chi_{c2})/\sigma(\chi_{c1})$ as a function of center-of-mass rapidity y^*, for the χ_{c2} and χ_{c1} promptly produced in pPb collisions measured using converted photons (red circles) and calorimetric photons (blue squares).

References

[1] K.J. Eskola, P. Paakkinen, H. Paukkunen and C.A. Salgado, *Towards epps21 nuclear pdfs*, 2021.

[2] *Lhcb detector performance*, *International Journal of Modern Physics A* **30** (2015) 1530022.

[3] LHCb collaboration, *The LHCb Detector at the LHC*, *JINST* **3** (2008) S08005.

[4] N. Armesto, *Nuclear shadowing*, *J. Phys. G* **32** (2006) R367 [hep-ph/0604108].

[5] K.J. Eskola, I. Helenius, P. Paakkinen and H. Paukkunen, *A QCD analysis of LHCb D-meson data in p+Pb collisions*, *JHEP* **05** (2020) 037 [1906.02512].

[6] I. Helenius and H. Paukkunen, *Double D-meson production in proton-proton and proton-lead collisions at the LHC*, *Phys. Lett. B* **800** (2020) 135084 [1906.06971].

[7] S. Cho and S.H. Lee, *Production of multicharmed hadrons by recombination in heavy ion collisions*, *Phys. Rev. C* **101** (2020) 024902 [1907.12786].

[8] R.J. Fries, B. Muller, C. Nonaka and S.A. Bass, *Hadronization in heavy ion collisions: Recombination and fragmentation of partons*, *Phys. Rev. Lett.* **90** (2003) 202303 [nucl-th/0301087].

[9] H.-S. Shao, *Probing impact-parameter dependent nuclear parton densities from double parton scatterings in heavy-ion collisions*, *Phys. Rev. D* **101** (2020) 054036 [2001.04256].

[10] LHCb collaboration, *Measurement of the relative rate of prompt χ_{c0}, χ_{c1} and χ_{c2} production at $\sqrt{s} = 7TeV$*, *JHEP* **10** (2013) 115 [1307.4285].